

## Trajectory-Dependent Neutralization of Low Energy $\text{Li}^+$ Scattered from Alkali Adsorbates on Ni(111)

L. Q. Jiang, Y. D. Li, and B. E. Koel

*Department of Chemistry, University of Southern California, Los Angeles, California 90089-0482*

(Received 21 December 1992)

Strongly trajectory-dependent neutralization is observed for low energy  $\text{Li}^+$  scattered from Cs adsorbed on Ni(111). For near glancing-exit scattering, the ion yield as a function of Cs coverage shows a pronounced peak and this behavior can be described well by a resonant charge-exchange model using the average work function. However, the yield is much smaller for near normal-exit scattering and the neutralization is mainly determined by the local electrostatic potential. Trajectory-independent, complete neutralization is observed at high coverages.

PACS numbers: 79.20.Rf, 34.70.+e, 79.90.+b, 82.65.My

Alkali-ion scattering is a powerful probe for real-space surface structure determination [1]. For surfaces with work functions much smaller than the ionization potential of the incident alkali, severe resonant neutralization occurs, which makes this technique unsuitable for the structure and site determination of alkali-covered surfaces. A quantitative understanding of the neutralization processes is of great interest for breaking this limitation and may offer a new measure of the local electronic structure at the surface, e.g., the charge state of the alkali adsorbate which is a controversial topic under much continued debate [2-4]. Charge exchange between an incident particle and the surface is also important in many dynamical processes such as molecular dissociation and chemisorption, as well as in various applications such as secondary ion mass spectroscopy, reactive ion etching, and ion beam deposition [5]. Because it is of such fundamental importance, this subject has attracted considerable theoretical and experimental effort [6,7]. Yet, the current literature has conflicting views as to whether the macroscopic work function or the local electrostatic potential is important for resonant neutralization processes.

Unlike the studies reported here, most previous ion scattering experiments did not observe scattering from the alkali adsorbates directly. For example, Geerlings, Kwakman, and Los [8] measured the charge fraction of various alkali ions scattered from Cs/W(110), but they could not distinguish whether the ion came from the substrate or the alkali adsorbate due to the lack of energy discrimination. While Kimmel *et al.* [9,10] did use an energy analyzer, they did not observe the scattering signal from alkali adsorbates, either because of the strong double scattering background or because their analyzer was not efficient enough. Similarly, German *et al.* [11] did not observe any features resulting from collision of  $\text{Li}^+$  with alkali adsorbates and concluded that nearly complete neutralization occurs for this process. In each case, these authors infer from their data that the local electrostatic potential is the key to understanding their results. On the other hand, the calculations by Zimny [12], treating the average work function as the key parameter, explained well the data in Ref. [8] without in-

voking a nonuniform local electrostatic potential. In addition, Ashwin and Woodruff [13] suggested that the average work function is the appropriate parameter of importance for resonant neutralization based on their data of  $\text{Li}^+ \rightarrow \text{Cs}/\text{Ni}(111)$ .

It is well established that the final charge state of a scattered alkali is determined along the outgoing trajectory. Whether resonant neutralization is determined by the average work function or local electrostatic potential may depend on the scattering geometry. Little progress has been made on this issue, possibly because previous studies were conducted either with a fixed scattering geometry [11,13] or with trajectories that varied only in a small range of angles near glancing [8] or  $45^\circ$  to the surface [9,10]. The scattered ion fraction in the latter cases did not reveal a strong and clear trajectory dependence also because scattering from the adsorbed alkali and the substrate was not distinguished. Not only is the ion yield for scattering from the substrate composed of contributions from substrate atoms that may have different neutralization probabilities depending on their distance from the alkali adsorbate, but it is also strongly influenced by angle-dependent shadowing and blocking effects. However, measurements of the ion yield for scattering from low coverage alkali adsorbates, which are far apart from each other within the adlayer, do not suffer from the ambiguity introduced by these complications.

In this Letter, we present ion scattering results for 0.2 and 1 keV  $\text{Li}^+$  from Cs-covered Ni(111) for outgoing trajectories near grazing as well as near normal to the surface. By using a large throughput hemispherical analyzer coupled with multichannel detection, we can observe scattering from alkali adsorbates directly. Our results indicate that neutralization for glancing-exit scattering depends mainly on the average work function, while for near normal-exit trajectories, it is mostly determined by the local electrostatic potential.

The experiments were carried out in a two-level UHV system. The upper level contains LEED optics, which were used as a retarding field analyzer for Auger electron spectroscopy and work-function-change measurements. The lower level contains a Colutron ion gun which pro-

duces mass filtered  $\text{Li}^+$  ions from a thermally activated  $\text{Li}^+$  source. The scattering experiments were performed using a Perkin-Elmer 280 mm spherical capacitor analyzer at a fixed scattering angle of  $144^\circ$ . The use of this large throughput analyzer coupled with a multichannel detector allows data collection with small ion doses, typically  $< 3 \times 10^{12}/\text{cm}^2$  per scan at a beam current density of  $\approx 15 \text{ pA}/\text{mm}^2$ . Ion beam damage was negligible under these conditions as evidenced by indistinguishable consecutive scans. The Ni(111) sample was cleaned by standard techniques. Fresh Cs films were deposited from well-degassed SAES getter for each coverage.

Figure 1 shows energy spectra of ion scattering from Cs/Ni(111). We have used the negative work-function change,  $-\Delta\phi$ , as a monitor of the Cs coverage,  $\Theta$ , because  $-\Delta\phi$  is very sensitive and directly proportional to  $\Theta$  at the low coverages of interest here. Figure 1(a) shows that the Cs single scattering peak intensity goes through a maximum with increasing Cs coverage for a near glancing exit angle of  $20^\circ$ . This is more clearly seen in the inset of Fig. 1(a) which shows an expanded view of the Cs peak. For a near normal exit angle of  $72^\circ$ , Fig. 1(b) shows that the Ni single scattering peak is on top of a much larger background due to multiple scattering which is more favorable in this scattering geometry than the one used for Fig. 1(a). With increasing Cs coverage, both the Ni single scattering peak and the background decrease while scattering from Cs is hardly seen on this scale. However, if we expand the Cs single scattering re-

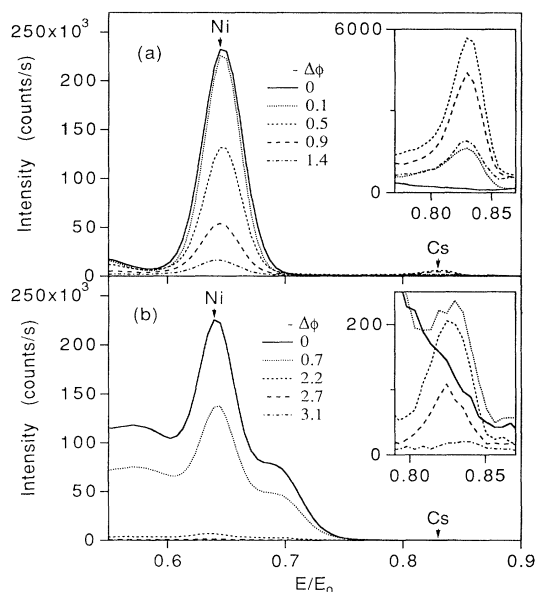


FIG. 1. Energy spectra from Ni(111) with various coverages of Cs as indicated by the Cs-induced work-function change, obtained with  $0.2 \text{ keV } ^7\text{Li}^+$  incident along the Ni [112] azimuth. (a) Exit angle of  $20^\circ$  relative to the surface plane; (b) specular scattering with a near normal exit angle of  $72^\circ$ . The insets show expanded views of the Cs single scattering region.

gion as shown in the inset of Fig. 1(b), the Cs single scattering peak is clearly seen to grow and then disappear. Complete neutralization is also observed for thick Cs films.

The Cs and Ni single scattering peak areas, integrated after removal of a linear background under each peak, are plotted as a function of  $-\Delta\phi$  in Fig. 2. The data for the two primary beam energies follow very similar trends and the much weaker scattering signal for  $E_0=1 \text{ keV}$  is mainly due to the smaller ion scattering cross section at higher energies. The trend in the Ni peak area with  $-\Delta\phi$  in Figs. 2(b) and 2(d) is very similar, monotonically decreasing to a small value at  $-\Delta\phi \approx 2 \text{ eV}$ . The importance of distinguishing ion scattering from the substrate and the adsorbed alkali is demonstrated by the Cs scattering yields which reveal striking differences for the two scattering geometries. For scattering with a near glancing exit angle of  $20^\circ$  relative to the surface, the Cs peak area shows a pronounced peak at  $-\Delta\phi \approx 0.5 \text{ eV}$  for  $E_0=0.2 \text{ keV}$  and at a noticeably larger  $-\Delta\phi$  of  $\approx 0.7 \text{ eV}$  for  $E_0=1 \text{ keV}$ . A subtle cutoff at  $-\Delta\phi \geq 2.8 \text{ eV}$  is seen and becomes apparent in the expanded view of this region shown in the inset of Fig. 2(a). The Cs peak areas shown in Fig. 2(c) are much weaker than those in Fig. 2(a) and they increase almost linearly with  $-\Delta\phi$  up to about  $2.0 \text{ eV}$ , and then drop to a vanishingly small value with a cutoff at  $2.8 \text{ eV}$ . In our studies of  $0.2 \text{ keV } \text{Li}^+ \rightarrow \text{K}$  on Ni(111), we also found that the ion yield for scattering from alkali adsorbates starts to drop at larger  $-\Delta\phi$  for near normal-exit scattering than for near glancing-exit scattering. We should point out that a couple of points near  $-\Delta\phi=3.0 \text{ eV}$  for  $E_0=0.2 \text{ keV}$  in Fig. 2 actually have coverages larger than that at  $-\Delta\phi=3.5 \text{ eV}$  (determined from Auger electron spectroscopy), and they correspond to monolayer and multilayer coverages of Cs that

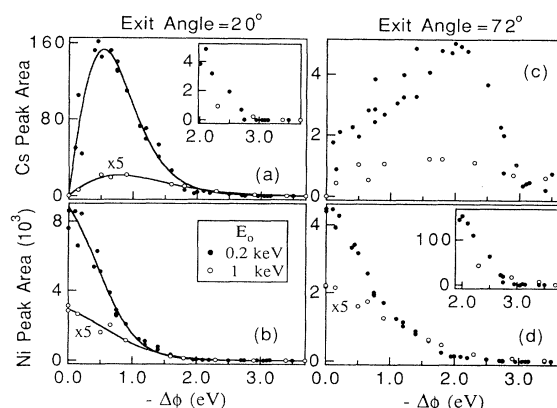


FIG. 2. Cs and Ni peak areas as a function of the Cs-induced work-function change. The left panels are for scattering with a near glancing exit angle of  $20^\circ$ . The right panels are for specular scattering with an exit angle of  $72^\circ$ . The insets show details for  $1.9 < -\Delta\phi < 3.7 \text{ eV}$ . The calculated results using the model described in the text are shown by the curves.

have passed the work-function minimum. Remarkably, the Cs peak areas in Fig. 2(c) are of similar magnitude as the cutoff region shown in the inset of Fig. 2(a). A cutoff in the Ni single scattering at the same value,  $-\Delta\phi \approx 2.8$  eV, is also seen in the inset of Fig. 2(d). This suggests that the cutoffs in all of the ion yields have a common origin that is independent of the scattering trajectory.

The analysis of the scattered ion fraction is often started with a semiclassical model for resonant neutralization [8,14]. This model rarely fits any data of scattering experiments including ours because it always predicts switching in the ion survival probability from unity at high work function to zero at low work function over a very narrow range of  $\approx 0.5$  eV. Following Geerlings, Kwakman, and Los [8], we have taken the Cs-induced local electrostatic potential into account and the model then predicts an ion survival probability of unity independent of Cs coverage for scattering with an exit angle of  $20^\circ$  and total neutralization for near normal exit scattering (exit angle  $=70^\circ$ ). This result may fit our data for  $-\Delta\phi \leq 0.5$  eV but it obviously fails to account for our data for  $-\Delta\phi > 0.5$  eV.

It is well known that the final charge state of a scattered alkali depends only on the outgoing trajectory. For a glancing-exit trajectory, the effects of adsorbate-induced corrugation in the local electrostatic potential on  $\text{Li}^+$  neutralization is expected to be averaged out by the large lateral interaction length due to the finite width of the capture process. Therefore, it is reasonable to use only the average work function and a model has been proposed recently for this case by Zimny [12]. Based on this model, the ion survival probability  $P^+$  can be approximated by

$$P^+ = \left[ 1 + 2 \exp \left( \frac{I - \phi - v^2/2 - 1/4z^*}{vv^*} \right) \right]^{-1}, \quad (1)$$

where  $z^*$  is the effective tunneling distance,  $v$  is the outgoing alkali velocity parallel to the surface, and  $I$  is the ionization potential of the alkali atom. The  $vv^*$  term represents the motional excitation of conduction electrons. Since  $-\Delta\phi \propto \Theta$  for the low Cs coverage range where most of the changes occur in Fig. 2 and the ion yield for scattering from Cs,  $I_{\text{Cs}}$ , is proportional to  $\Theta$  and  $P^+$ , we can write  $I_{\text{Cs}} = -a\Delta\phi P^+$ . Similarly  $I_{\text{Ni}} = \beta(1 + \gamma\Delta\phi)P^+$ , where the  $\gamma\Delta\phi$  term takes into account the shadowing and blocking effects of adsorbed Cs on the scattering from Ni. Using  $I = 5.39$  eV for Li and  $\phi = 5.35$  eV for clean Ni(111), we can then apply these expressions to fit the data in Fig. 2. Satisfactory results are obtained, as shown by the solid curves in Fig. 2, with  $z^* = 9.4a_0$  ( $a_0$  is the Bohr radius),  $vv^* = 0.30$  eV for  $E_0 = 0.2$  keV, and  $z^* = 8.0a_0$ ,  $vv^* = 0.50$  eV for  $E_0 = 1$  keV. The value of  $z^*$  can also be calculated from  $\Delta_0 \exp(-az^*) = av_z$ , where  $v_z$  is the velocity component of the scattered Li normal to the surface,  $\Delta_0$  and  $a$  are the preexponential factor and decay constant for the

width of the Li ionization level [15]. Using the values for  $\Delta_0$  and  $a$  given in Ref. [8], we found the value of  $z^*$  to be  $8.8a_0$  and  $8.0a_0$  for  $E_0 = 0.2$  and 1 keV, respectively. The peaking of  $I_{\text{Cs}}$  at larger  $-\Delta\phi$  in Fig. 2(a) for larger  $E_0$  is due to the smaller value of  $z^*$  at higher energy. The agreement between the calculated value of  $z^*$  and those obtained from fitting the experimental data further supports Zimny's model for resonant neutralization in describing scattering with a near glancing outgoing trajectory using the work function as the key parameter. Note, however, the preexponential factor 2 in Eq. (1) will be replaced by 1 if the spin degree of freedom is neglected. In this case, the same quality fit to the data for  $E_0 = 0.2$  keV requires  $z^* = 13.3a_0$ , which is unreasonably large at this energy. It is thus evident that the electron spin degree of freedom is important in describing the resonant charge-exchange process.

Since specular scattering with near normal-exit geometry occurs mainly on top of the atom that the incident ion strikes, the local electrostatic potential due to the Cs-induced dipole moment  $p$  may play an important role in the neutralization of  $\text{Li}^+$  scattered from Cs. The effect of an inhomogeneous electrostatic potential in resonant neutralization has been considered in earlier studies [8-11,14]. The ionization level of Li will be shifted down in energy as the outgoing Li passes at a distance  $r$  from the dipole center by an amount  $p \cos\theta/r^2$  where  $\cos\theta = z/r$ . Assuming a dipole moment of  $4 \times 10^{-29}$  Cm as used in Refs. [8] and [13], the magnitude of this downward shift will be larger than the upward image shift of  $1/4z$  for  $z \leq 10 \cos^3\theta \text{ \AA}$ . While this range is too small to influence the near glancing-exit scattering with  $\theta = 70^\circ$ , it will cover  $z^*$ , where resonant neutralization is most effective, for near normal-exit scattering with  $\theta = 18^\circ$ . This explains the much smaller peak areas in Fig. 2(c) compared to Fig. 2(a), and their drop at larger  $-\Delta\phi$  is because the dipole potential does not vary much with low Cs coverage. Thus for near normal-exit scattering, the neutralization is mainly determined by the local electrostatic potential. The fact that scattering from Cs is not completely neutralized and the fast decrease in  $I_{\text{Ni}}$  with  $-\Delta\phi$  indicates that, in contrast to German *et al.* [11], the neutralization is not site specific and is enhanced also at Ni sites near adsorbed Cs. This result is also obtained in our studies of  $\text{Li}^+ \rightarrow \text{K/Ni}(111)$ .

The strongly trajectory-dependent neutralization of  $\text{Li}^+$  scattered from Cs/Ni(111) is further evidenced by the effects of oxygen on Cs peak areas. Figure 3(b) shows that  $I_{\text{Cs}}$  greatly increases following oxygen adsorption for all initial Cs coverages. This can be understood naturally using the local view for this scattering geometry: The Cs-O bond formation changes the electrostatic potential (increases the local work function) near Cs. Meanwhile, for scattering with a glancing exit angle of  $20^\circ$ , Fig. 3(a) shows that  $I_{\text{Cs}}$  is almost independent of the same doses of oxygen for  $-\Delta\phi < 0.5$  eV and increases only for higher initial Cs coverages following oxygen ad-

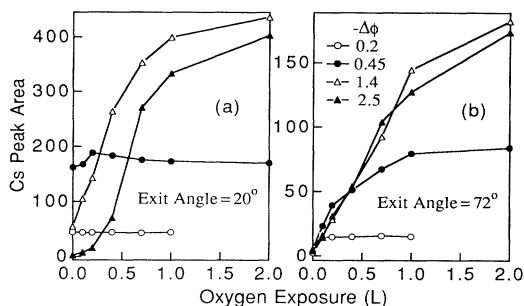


FIG. 3. Cs peak areas ( $E_0=0.2$  keV) as a function of oxygen exposure for two scattering geometries: (a) exit angle of  $20^\circ$  and (b) exit angle of  $72^\circ$ . The Cs-induced work-function change is used to monitor the Cs coverage. ( $1 \text{ L}=10^{-6}$  Torrsec.)

sorption. Since  $-\Delta\phi < 0.5$  eV corresponds to a coverage range where the ion fraction is still high, as shown by the rise in  $I_{\text{Cs}}$  with  $-\Delta\phi$  in Fig. 2(a), increasing the work function by oxygen adsorption will not have much effect. On the other hand, for  $-\Delta\phi = 1.4$  or  $2.5$  eV, the drop in  $I_{\text{Cs}}$  with  $-\Delta\phi$  in Fig. 2(a) indicates severe neutralization, and thus increasing the work function by oxygen adsorption reduces the neutralization and increases  $I_{\text{Cs}}$  drastically. These data provide additional support for the conclusion that the neutralization depends on the work function for glancing-exit scattering while the variation in local electrostatic potential must be considered for scattering with a near normal outgoing trajectory.

Since a cutoff near  $2.8$  eV is observed in Figs. 2(a), 2(c), and 2(d), this feature is not trajectory dependent and must be correlated to a change in the surface electronic properties. The  $\text{Li}^+ \rightarrow \text{Cs}$  scattering yield in Fig. 2(c) starts to fall near  $2.1$  eV, just about the point where the  $-\Delta\phi$  vs  $\Theta$  curve begins to deviate from linearity. This suggests that a decrease in the polarization or a change in the charge state of the adsorbed Cs due to depolarization effects possible at these coverages causes more electron density to be available for charge transfer to  $\text{Li}^+$  in addition to the continually decreasing work function that will also increase neutralization. The  $\text{Li}(2p)$  level also starts to cross the Fermi level at this work-function range so that some population of excited neutral Li may contribute to the drop in  $\text{Li}^+$  yield, and at even lower work function, negative ion formation may also become possible. It should be pointed out that the local electrostatic potential and average work function views may become equivalent at these coverages. Indeed, the Cs peak areas in Fig. 2(c) are comparable in magnitude to those of Fig. 2(a) for  $-\Delta\phi \geq 2$  eV. It is not surprising that  $I_{\text{Ni}}$  in Fig. 2(b) drops to zero at smaller  $-\Delta\phi$  than the cutoff point because, in addition to neutralization effects, Ni atoms are more effectively shadowed and blocked by Cs with this near glancing-exit scattering geometry.

Ashwin and Woodruff [13] have reported  $1$  keV  $\text{Li}^+$

scattering from Cs/Cu(110) with a scattering geometry very similar to our specular scattering with near normal-exit trajectories. However, they observed that  $I_{\text{Cs}}$  increases with coverage initially and then, instead of dropping to zero as in our study, it decreases slightly prior to rising again up to monolayer saturation. They did not study the  $\text{Li}^+ \rightarrow \text{Cs}$  scattering from multilayer Cs films due to the lack of cooling in their experiments. Our observation of complete neutralization for monolayer and multilayer Cs is incompatible with their result. We found that if the Cs/Ni(111) sample sat for a long time even in a vacuum of  $1 \times 10^{-10}$  Torr or if a number of scattering experiments were performed,  $I_{\text{Cs}}$  was significantly larger than for a fresh sample. The studies shown in Fig. 3 and similar experiments for CO clearly show that small amounts of coadsorbates can increase  $I_{\text{Cs}}$  drastically. This is why we prepared a fresh sample for scattering experiments at each Cs coverage. The results of Ashwin and Woodruff were obtained by adding successive doses of Cs, in a somewhat worse vacuum than ours. Therefore we believe that their results were most likely influenced by coadsorbed impurities and/or ion-induced damage.

In conclusion, we report the first detailed measurements of low energy  $\text{Li}^+$  ion scattering from alkali adsorbates and we demonstrate that the  $\text{Li}^+$  ion fraction from alkali covered surfaces is strongly trajectory dependent. The scattered ion fraction is determined by the average surface work function for glancing-exit trajectories, while it is influenced by the local electrostatic potential for near normal outgoing trajectories.

This work was supported by the Division of Chemistry, National Science Foundation.

- [1] E. Taglauer, in *Ion Spectroscopies for Surface Analysis*, edited by A. W. Czanderna and D. M. Hercules (Plenum, New York, 1991), pp. 363-416, and references therein.
- [2] G. A. Benesh and D. A. King, *Chem. Phys. Lett.* **191**, 315 (1992).
- [3] M. Scheffler *et al.*, *Physica* **172B**, 143 (1991).
- [4] D. M. Riffe, G. K. Wertheim, and P. H. Citrin, *Phys. Rev. Lett.* **64**, 571 (1990).
- [5] S. R. Kasi *et al.*, *Surf. Sci. Rep.* **10**, 1 (1989).
- [6] R. Brako and D. M. Newns, *Rep. Prog. Phys.* **52**, 655 (1989).
- [7] J. J. C. Geerlings and J. Los, *Phys. Rep.* **190**, 133 (1990).
- [8] J. J. C. Geerlings, L. F. Tz. Kwakman, and J. Los, *Surf. Sci.* **184**, 305 (1987).
- [9] G. A. Kimmel, D. M. Goodstein, and B. H. Cooper, *J. Vac. Sci. Technol. A* **7**, 2186 (1989).
- [10] G. A. Kimmel *et al.*, *Phys. Rev. B* **43**, 9403 (1991).
- [11] K. A. H. German, C. B. Weare, P. R. Varekamp, J. N. Andersen, and J. A. Yarmoff (to be published).
- [12] R. Zimny, *Surf. Sci.* **233**, 333 (1990).
- [13] M. J. Ashwin and D. P. Woodruff, *Surf. Sci.* **244**, 247 (1991).
- [14] R. Brako and D. M. Newns, *Surf. Sci.* **108**, 253 (1981).
- [15] E. G. Overbosch, B. Rasser, A. D. Tenner, and J. Los, *Surf. Sci.* **92**, 310 (1980).